PM fiber lasers at 589nm: a 20W transportable laser system for LGS return flux studies

Domenico Bonaccini Calia[1], Axel Friedenauer[2], Vladimir Protopopov[3], I.Guidolin[1], Luke R. Taylor[1], Vladimir I. Karpov[3], Manfred Hager[2], Wallace R. L. Clements[3], Bernhard Ernstberger[2], Steffan Lewis[1] and Wilhelm G. Kaenders[2]

[1] Laser Systems Department, ESO, Karl-Schwarzschild-Str. 2, D-85748 Garching, Germany – www.eso.org

[2] TOPTICA Photonics AG, Lochhamer Schlag 19, D-82166 Graefelfing, Germany - www.toptica.de

[3] MPB Communications Inc., 147 Hymus Boulevard, Montreal, Quebec H9R 1E9, Canada - www.mpbc.ca

ABSTRACT

In this paper we present the rationale and design of a compact, transportable, modular Laser Guide Star Unit, comprising a 589nm laser mounted on a 300mm launch telescope, to be used in future experiments probing the mesospheric sodium properties and to validate existing LGS return flux simulations. The 20W CW 589nm Laser is based on the ESO developed concept of 589nm lasers based on Raman Fiber Amplifiers, refined and assembled together with industry. It has the same laser architecture as the laser which will be used for the VLT Adaptive Optics Facility. We have added to the 20W CW laser system the capabilities of changing output polarization, D_{2b} emission levels, power level, linewidth and to operate as pulsed laser with amplitude modulation. We focus in this paper on the laser description and test results.

Keywords: Laser guide stars, fiber lasers, sodium return flux

1. INTRODUCTION

In the past years ESO together with the group of Prof. Budker at Berkeley has produced to our knowledge the most refined model of the sodium LGS return flux, with the aim to define the laser properties which give the best return flux [1], in view of the VLT AOF and E-ELT projects, both of which will use multiple Laser Guide Stars (LGS). Measurements of LGS return flux varying the relevant laser parameters are required to validate these simulations, as there are very few calibrated LGS return flux measurements available, while consistent return flux gains are anticipated by the simulations if the proper laser format is selected [6].

Moreover, with the design of extended and complex LGS-AO systems there is a general need for specific field experiments on system issues affecting the designs, like the mesospheric sodium abundance [4], the sodium profile variability [3, 5], the different elongated geometries on wavefront sensors sub-apertures produced by monostatic and bistatic propagation schemes [7], the effectiveness of spot tracking with pulsed lasers and the fratricide effect, only to name the most relevant ones.

Building on the successful development of the ESO Fiber Raman Amplifier (EFRA) and of a compact 589nm fiber laser in the past 5 years [10] as well as on the recent progress of the laser industry with such developments, ESO is assembling a transportable LGS Unit (LGSU) as tool to carry on strategic LGS field experiments (*Figure 1*). The LGSU consists of a 20W CW, 589nm laser system, whose main subsystems have been assembled by the laser industries Toptica AG and MPB Communications Inc., directly attached to a steerable refractive launch telescope produced by Astelco Systems GmbH. The uplink laser beam is 300mm in diameter. The laser has been assembled and tested in the past six months, while the launch telescope mechanical parts and optics have been produced and have still to be assembled at the time of this writing.

It must be noted that for this experimental setup both the laser system and the launch telescope optics have designs rather similar to those adopted for the VLT 4LGSF/AOF system [8,9], which is undoubtedly an asset enabling to spot early on problems or design issues and to validate, during the commissioning phase and in the field experiments, several design aspects of the 4LGSF laser and launch telescope systems before they will be manufactured.

The main goal of this paper is to report on the design and performance of the compact fiber laser subsystem of the LGSU. The laser head attached to the launch telescope occupies a volume of 500x350x105mm^3, and the attached polarization-maintaining (PM) Raman Fiber Amplifier (RFA) occupies an additional volume of a cylinder with a base of 350mm in diameter and 150mm in height.

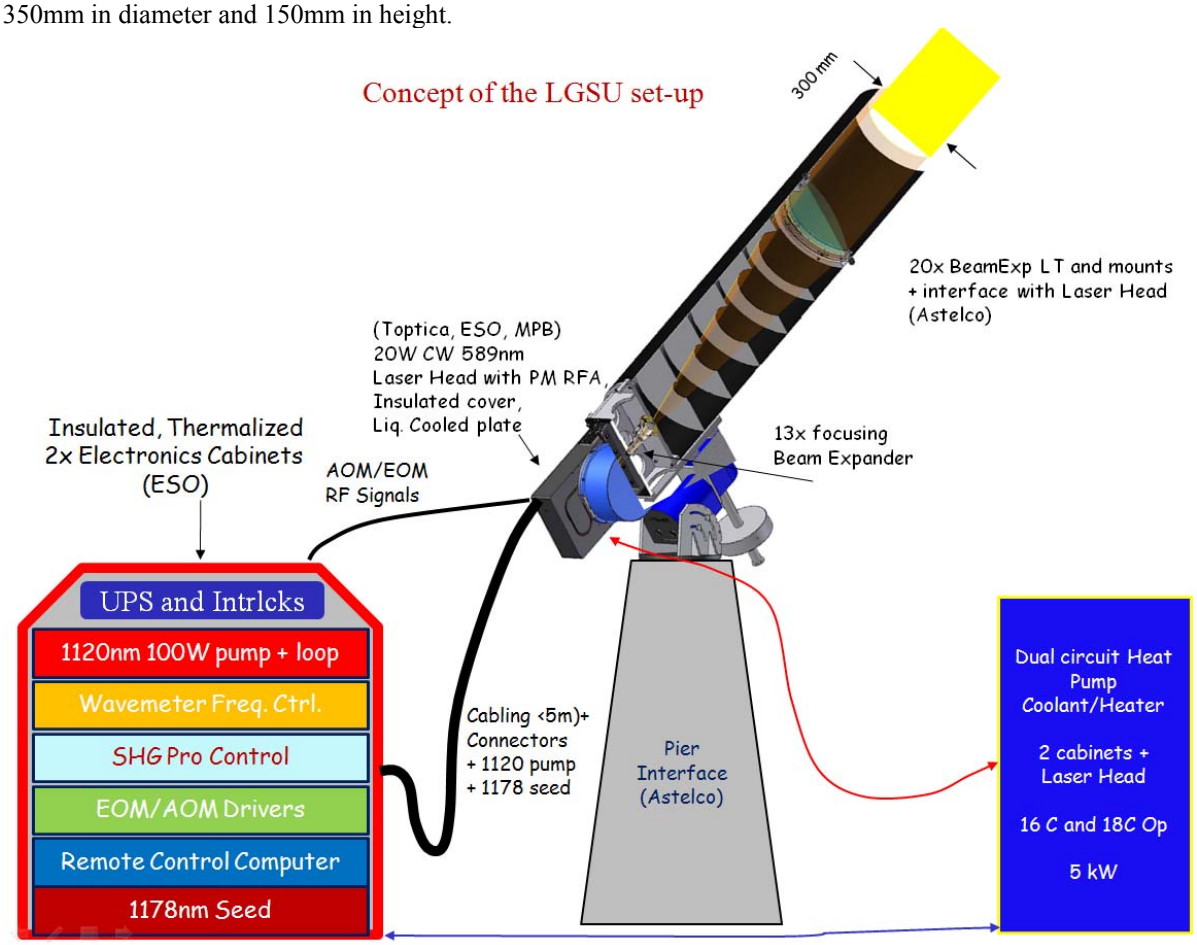

Figure 1: The ESO Laser Guide Star Unit consists of two electronics cabinets, 800x600x1600 mm, one laser head with the 1178nm narrow-band Raman Fiber Amplifier, 500x350x255mm, both attached to the bottom of a refractive launch telescope, 1600mm long producing a 300 mm diameter uplink laser beam.

1.1 Scientific targets

The laser power specifications for the AOF/4LGSF system, and for the Phase B study of the E-ELT, are based on the results of our numerical simulations on return flux, which predict to meet the Adaptive Optics return flux specifications with a 20W CW laser if an enhanced return flux is obtained by means of circular polarization of the laser beam, linewidth of 5 MHz and efficient D_{2b} re-pumping. It is rather important and strategic to validate the return flux simulations experimentally, in the coming two years.

We need as first priority to tackle the dependencies of the LGS returns flux from the laser emission formats and the pointing direction (impact of the alignment of the laser beam with the Earth's magnetic field lines, see [5]). Different experiments are foreseen:

1. The efficiency of the optical pumping is reduced by the sodium atom Larmor precession induced by the geomagnetic field. The orientation between the geomagnetic field line and of the laser propagation vector influences the return flux. The return flux expected e.g. in Paranal is indicated in Figure 2, in units of

10^6ph/s/m^2, for circularly polarized light and with re-pumping at 12%. The plot takes into account the effect of air-mass. When pointing the LGS in the direction of the white dot in Fig.2, the earth magnetic field B is parallel to the light propagation vector and the optical pumping is optimal. See also [6] for more details. In the related experiment we will measure the return flux pointing the LGS for different LGS pointing directions on the sky, varying the ALT-AZ of the launch telescope pointing, with optimal re-pumping and at maximum power output. For each pointing we will measure the return flux varying the polarization state of the laser beam, from linear to elliptical, to circular.

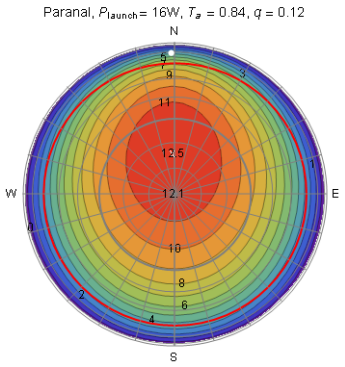

Figure 2: return flux in 10^6 ph/s/m^2, as a function of ALT and AZ at Paranal. The plot center is Zenith, the edge is the horizon.

2. The return flux dependence from the CW laser linewidth, according to our simulations, should have a maximum at L= P/6, where P is the power in air, L is the linewidth in MHz. The laser should be able to vary the linewidth at least between 5 and 20 MHz. The return flux variation vs laser linewidth curve is given in [1].

3. The efficiency of the optical pumping depends on the intensity, or power density, of the LGS at the mesosphere [2]. Varying the LGS size by changing focus, a scan of the power density can be produced, which will result in a variation of the return flux. This is illustrated in Figure 3 and detailed in [1]. The LGS spot size at the mesosphere will be derived experimentally, see point (5.) below

4. In the absence of saturation, the LGS return flux should be proportional to the emitted power. The curve of the return flux vs emitted power and light polarization will allow determining the onset and presence of saturation, for different polarization states.

5. The LGS spot size will be derived by imaging simultaneously on the same detector an NGS photometric calibrator star in V-band and the LGS, around the LGS pointing coordinates. The NGS image will be deconvolved from the LGS image obtained on the same detector, to derive the mesospheric LGS.

6. $D2_b$ re-pumping should increase the return flux by factors up to 3-4 in Paranal, with 16W of laser power in air. The variation of the return flux vs the fraction of the power emitted in the $D2_b$ line will be experimentally verified. See [1] for more details.

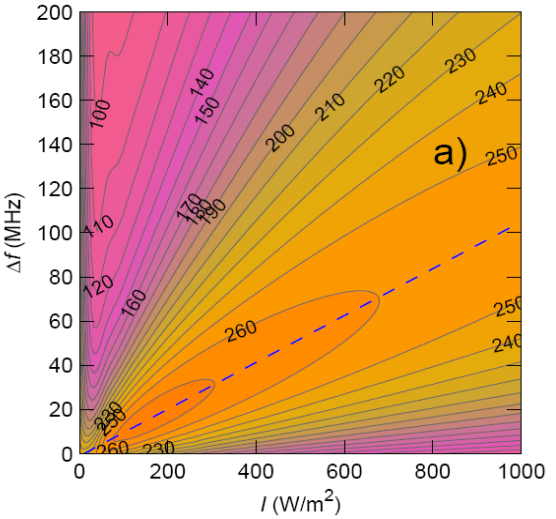

Figure 3: dependence of the return flux from the linewidth and the LGS intensity at the mesosphere. The contours values are proportional to the return flux

Three more areas of R&D related to LGS are targeted by our development of the LGSU:

- The validation of the latest results on the fast variability of the mesospheric Sodium layer [3].
- Field experiments on elongated spot wavefront sensing and on LGS spot tracking, via the creation of suitable 5 microseconds pulse formats (via amplitude modulation) [7]

1.2 Laser Main Requirements

The requirements are derived for the experimental system, in order to test the return flux sensitivity to the emitted polarization, laser linewidth, D_{2b} re-pumping levels, pulsed operation (amplitude modulation), and to operate directly attached to the launch telescope. For the laser:

Laser Main Requirement	Value/definition
Laser Head location	attached to Launch Telescope
Laser Head can operate with varying gravity vector	operation ALT 20-90º
Laser linewidth	<5 MHz
Possibility to change the linewidth electronically	Up to 20 MHz
Laser Power	20 W CW at 589nm
Frequency control stability	±40 MHz
Laser beam optical quality	< 50 nm rms
Output beam waist w_o	1.1±0.1 mm in diameter, located at laser exit ±2m
Output beam polarization	PER > 50:1
Possibility to change the polarization state online. Polarization Ellipticity resolution	±0.02
Output Beam Stability (decenter, tilt)	100 μm radius, 1 arcmin tilt
Laser power monitors	Relative power, measured at 1178 nm and 589 nm
Emitted line profile monitor	2.5 MHz resolution, range <1000 MHz
Sideband spectrum for D_{2b} re-pumping	1.713 GHz from D_{2a}
Sideband amplitude for D_{2b} re-pumping	amplitude adjustable, up to 15% of D_{2a} intensity
Amplitude Modulation	Adjustable, up to 660 kHz, extinction < 1%
Distance of laser electronic cabinet from laser head	≥ 3m

1.3 Launch Telescope Main Requirements

Launch Telescope Main Requirement	Value/definition
Design type	Athermalized Refractor, 20x Beam Expander
Output Beam Diameter	300 mm
Pointing Coordinates and Range	ALT/AZ: ALT 0-90º, AZ ±180
Pointing accuracy	<5 arcsec in operating range
Optical Quality including BEU (tilt and focus removed)	WFE < 85 nm rms
Throughput	> 92%
Focus Range	70-200 km
Polarization Loss	<3%

2. THE 20W LASER

2.1 The 1178nm module MOPA Scheme

The laser is based on a master oscillator-Power Amplifier scheme (MOPA), in which a narrow band seed laser at 1178nm drives a 40W 1178nm polarization maintaining Fiber Raman Amplifier (RFA), in-line pumped by a 100W, 1121 nm commercial fiber laser (Figure 4). From the output of the seed to the end of the 1178nm module, no free space components are used, the 1178nm high power laser output is from a single-mode fiber core.

Both the 1178nm seed laser and the 1121 nm 100W CW pump fiber laser are placed in the laser electronics cabinet and connected via armored-protected, single mode fibers to the RFA at several meters distance. The power dissipation in the laser head is of the order of 60W and it is removed by thermal contact with the water cooled laser head.

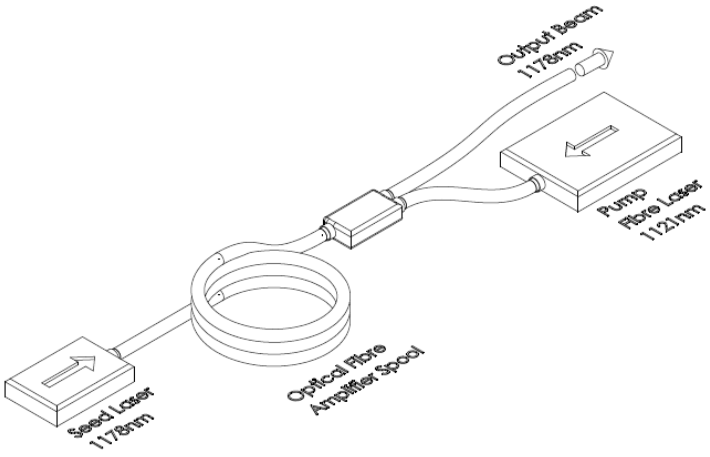

Figure 4: MOPA scheme of the PM 40W 1178nm laser source, pumped by a 100W CW commercial fiber laser at 1121nm

2.2 The Second Harmonic Generation

The second harmonic generation (or frequency doubling) process produces one photon at 589 nm for every two photons at 1178 nm, in our laser via a non-linear crystal inserted in a resonant cavity. The fiber output of the 1178 nm RFA is collimated in the Laser Head, containing a high power optical isolator and the mode-matching optics (lenses and mirrors) to feed the frequency doubling resonant cavity (Figure 5). The compact, commercially available SHG-pro ring resonant cavity is controlled via a Pound-Drever-Hall scheme and uses LBO as non linear crystal for the frequency conversion. The good beam quality of the 1178 nm source and the extremely low passive cavity losses, allow reaching SHG optical conversion efficiencies better than 80%.

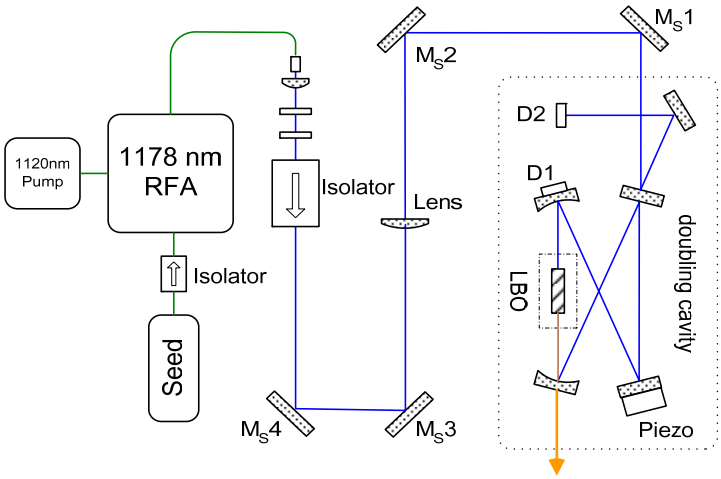

Figure 5: the 1178nm fiber laser feeds a Toptica SHG-pro frequency doubling resonant cavity based on the LBO crystal, which converts each two photons at 1178 nm into one at 589 nm.

Besides the PDH cavity control loop, the laser control scheme includes wavelength stabilization using a commercial wavelength meter with a precision of ±10 MHz, a reference stabilized low-power laser and working in closed feedback loop on the 1178nm seed laser, at a rate of 15 Hz (Figure 6).

This control scheme is based on commercially available components, most of which were used during former laser development at ESO, and have been now implemented in the LGSU laser head.

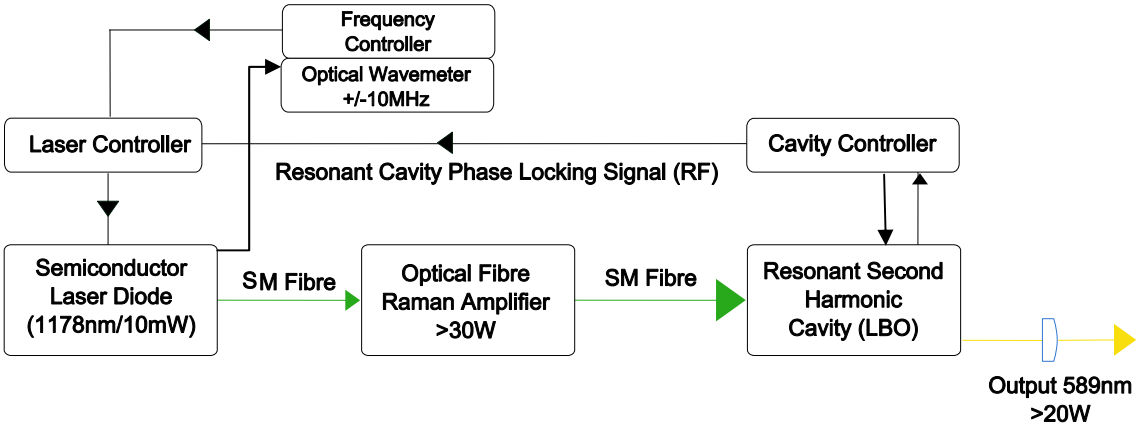

Figure 6: Laser scheme including the two control loops, for the frequency stabilization and the frequency doubling unit.

2.3 The Laser Head

The water-cooled laser head accommodates the SHG unit, an Electro-Optical Modulator (EOM) to generate the line sidebands at 1.713 GHz (D_{2b}), an Acousto-Optic Modulator (AOM) acting as fast beam deflector to generate amplitude modulation, and a quarterwave – halfwaveplate in series, which can be rotated remotely to generate arbitrary output polarization states. The Laser Head hosts a mirror shutter, various power monitoring diodes and a temperature sensor.

This illustrated schematically in Figure 7. The focusing Beam Expander is placed outside the Laser Head, and used to produce a 15 mm beam as input to the Launch Telescope. The coolant is kept at 18±1 °C and thermal insulation is used to shield the Laser Head from the environment.

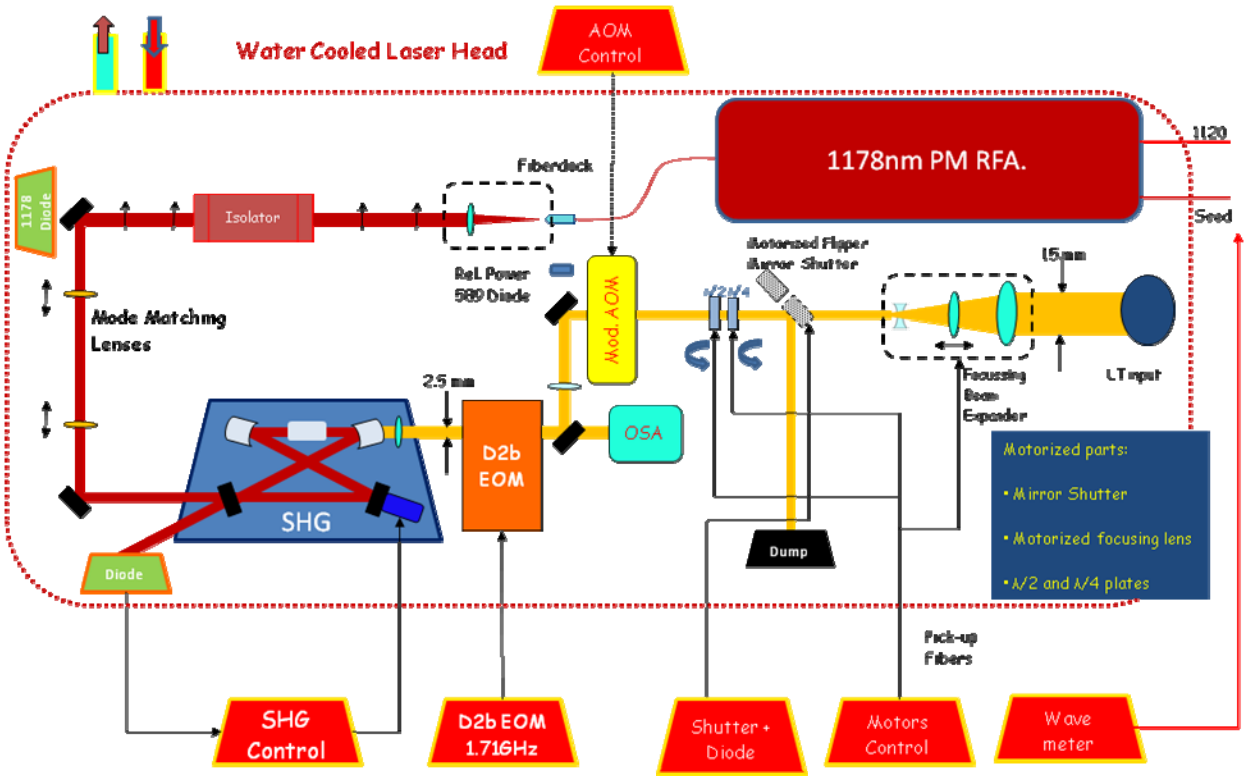

Figure 7: Diagram of the Laser Head and its functionalities. After the SHG unit an EOM and AOM can be used to produce re-pumping and amplitude modulation for pulsed operation. The AOM zero-order signal is dumped.

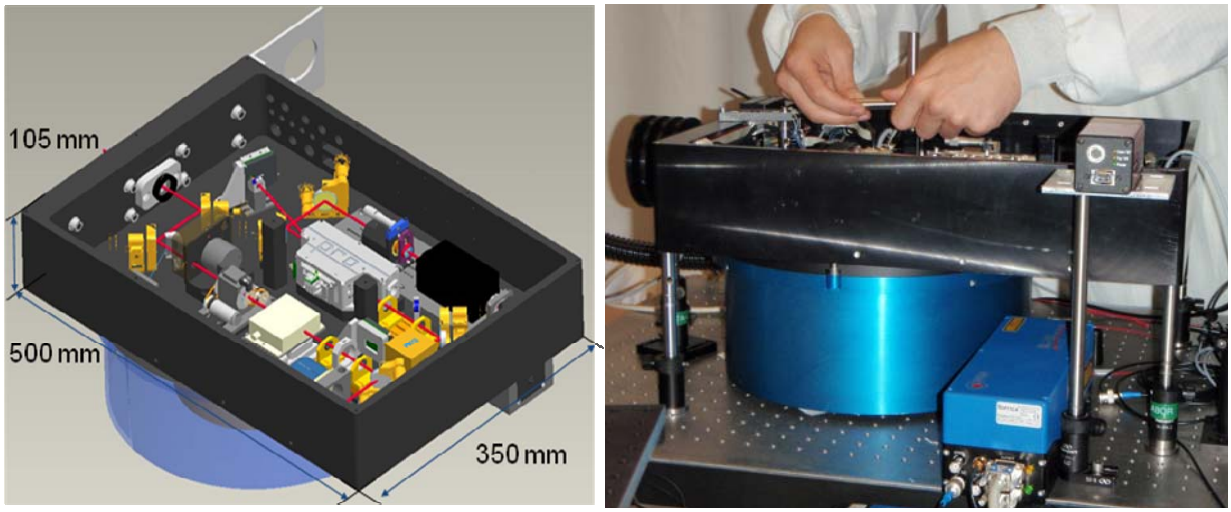

Figure 8: The 500x350x105 mm^3 laser head is water cooled at 18±1 °C and has the RFA attached on the bottom. The RFA is cooled by thermal contact with the laser head baseplate. On the right, a picture taken during the integration.

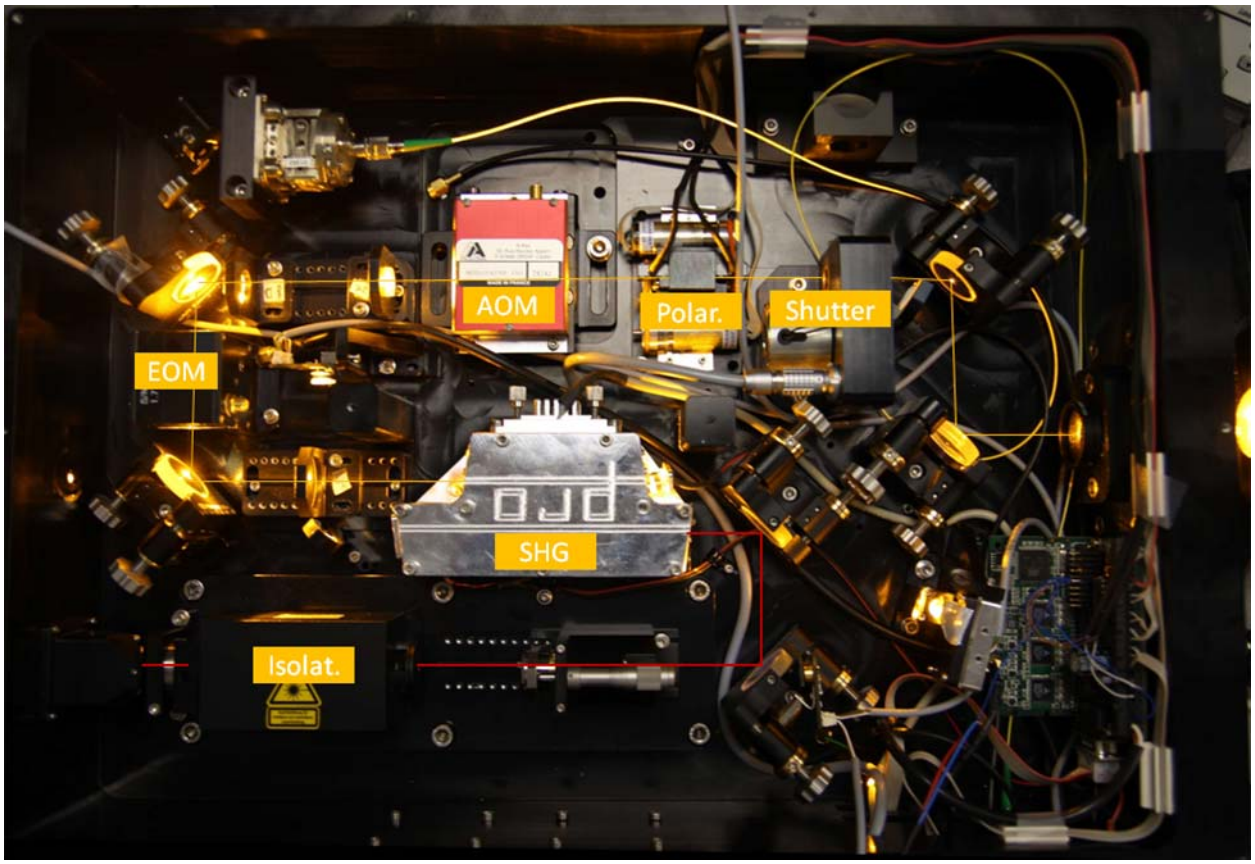

Figure 9: Laser Head top view. The 1178 nm free space beam enters from the bottom left side passing through the isolator, the mode matching telescope and two folding flats, before entering the SHG Pro unit. The 589 nm beam exiting the SHG-pro is folded and spatially matched first to the EOM and then to the AOM, before reaching the motorized polarization control and the shutter. Two further folding flats are used to align the output beam to the exit port, which is to the right in the picture.

2.4 The Electronics

Two water-cooled cabinets with high EMI isolation have been built by ESO, to control the laser (laser cabinet), to provide the RF drivers for the modulators, the interlocks system and to provide the launch telescope functionalities (electronics cabinet). An industrial PC supervisory computer is integrated in the electronics cabinet, with the system control SW based on Labview. Via LAN a remote desktop can connect and operate the entire LGSU remotely.

The total power consumption of the LGSU is 4.5 kW at 380VAC. A double-circuit chiller system produces the cooling capacity for the two electronics cabinet at 16 °C, and the stabilized cooling for the laser pump and the laser head, at 18 °C.

An UPS is installed with >15min autonomy, to allow a smooth shut down of the laser in case of power failures. The cabinets can be pre-heated to warm up the subsystems in chilly environments, before a cold-startup of the system.

The system interlocks installed are:

1. Laser protection interlock on RFA Stimulated Brillouin Scattering
2. Laser protection interlock on 1120 pump power-drop
3. Laser protection interlock on 1178nm seed power drop
4. Propagation shutter interlock from remote aircraft spotter switch

Figure 10: Electronics cabinet with the EOM RF driver, the integrated PC computer, the interlock panel, the EOM and AOM RF generators

3. 20W 589NM LASER TEST RESULTS

3.1 1178nm PM RFA

3.1.1 PM RFA Emission Specifications and Monitored Signals

Parameter	Units	Min	Nom	Max	Comments
Output Power Per Channel	W	10	36	37	
Adjustable Power Range	%	50		105	% of nominal
Amplification Wavelength	nm	1176	1178	1179	
Linewidth	MHz	2	4	25	
RIN	%			4	RMS, 5Hz-1MHz

Monitor	Access to monitored parameter	Tap Ratio/ Response	Conditions
Backward SBS	Optical via fiber tap	1%	Pump is On
Output RFA power	via electrical cable	100mV/W (Gain low)	Pump is On
Pass through signal (at the RFA output)	via electrical cable	10mV/mW (Gain high)	Pump is Off
Delivered pump power	Optical via fiber tap	0.086mW/W	Pump is On

Using a single-arm RFA approach up to 44W at 1178 nm have been produced with a 100W, 1121 nm pump. To produce 20W at 589 nm, 32W are required from the RFA output, before the optical isolator. We have therefore some margin and

do not have to operate the laser pump at its maximum. The plot in Figure 11 shows the RFA output power at 1178 nm as a function of the pump laser power at 1121 nm (circles). The squares show the SBS signal level. The RFA is interlocked if the SBS power goes above 0.2W. The test results demonstrate that the PM RFA is meeting and exceeding the output power specifications.

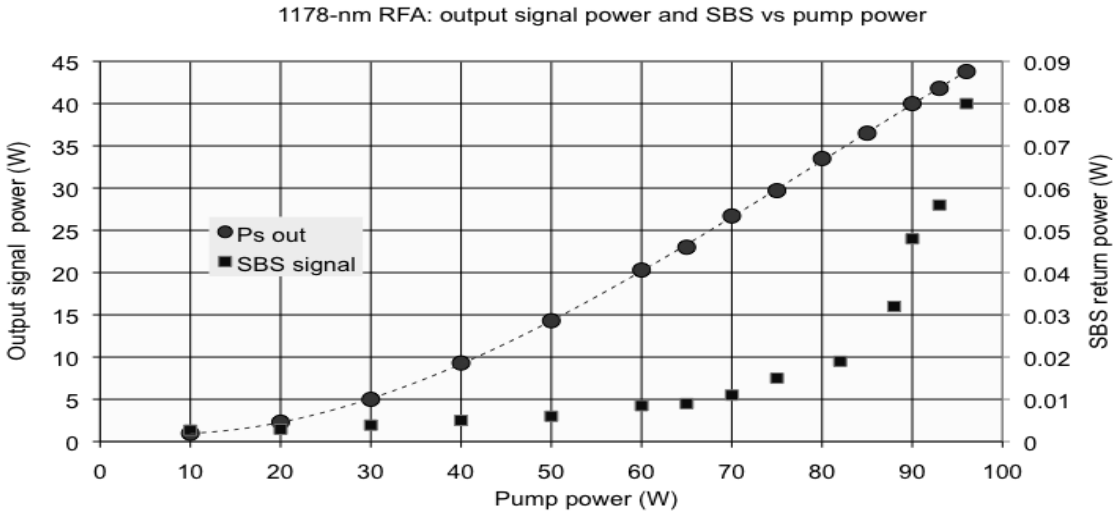

Figure 11: 1178nm RFA power output (circles, left ordinate axis) as a function of the pump power. SBS (squares, right ordinate axis) generated at the same pump power level. The RFA output power specification is 36W, operation at 32W CW. Up to 44 W power has been demonstrated with stable operation during the tests.

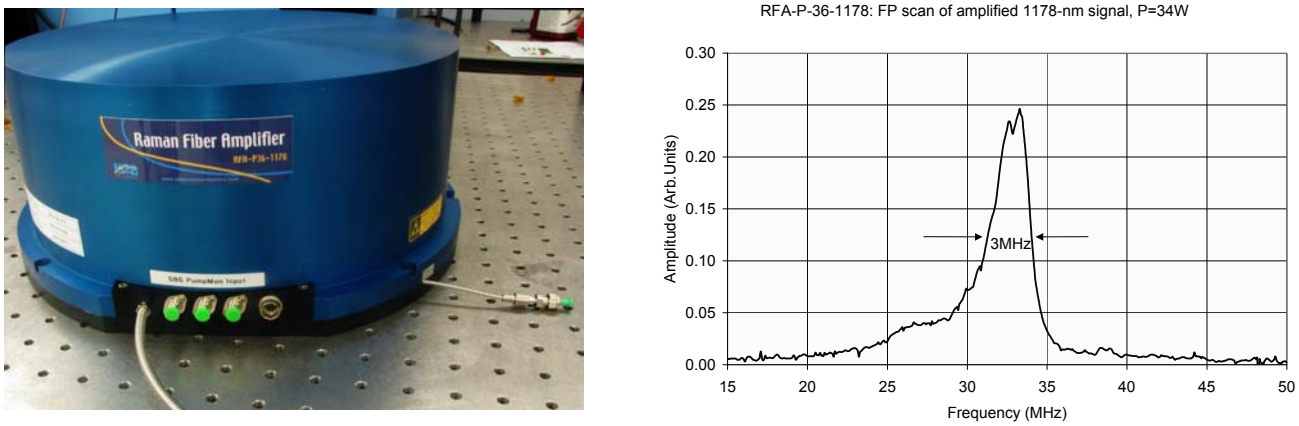

Figure 12: Left: picture of the RFA as delivered from MPBC; Right: spectrum of the emitted line taken with an IR Optical Spectrum Analyzer, at RFA power of 34W. The line profile asymmetry is due to the spectrum analyzer misalignment.

The 1178 nm emitted line was taken at 34W using an infrared Optical Spectrum Analyzer (OSA) and it is shown in Figure 12. The linewidth measured is 3 MHz, however the OSA Finesse is limiting the resolution and the slight misalignment of the Fabry Perot influences the symmetry of the result. The specification on relative intensity noise was equally met, with an rms of 0.4% measured in the frequency range 5 Hz-1 MHz, 10 times better than specifications.

The RFA met all technical specifications, it has no movable parts or free space optics and hence it is not influenced by the gravity vector changes when it will be attached to the Launch Telescope. The thermal management of some high power components is an area which will be further checked and improved before deploying the unit for field tests.

3.2 Second Harmonic Generation Tests

In the Laser Head the SHG-Pro cavity generates the 589nm photons. The 1178nm power entering the ring cavity is lower than the RFA output due mainly to the absorption of the free space beam in the infrared Optical Isolator. The measured optical conversion efficiency is obtained by the ratio of the cavity input and output powers. Adjusting the mode matching of the input beam to compensate the optical isolator thermal lensing, we have obtained consistently efficiencies above 80% (see Figure 13).

The emitted spectral line was measured using an OSA for the visible with a spectral resolution of 2MHz, at 589 nm laser power levels of 10, 15 and 20 W, with the EOM activated to produce the D_{2b} sidebands at 1.713 GHz having 10% of the central emission line peak intensity, as specified.

In case the RFA would experience Four-Wave Mixing, we would observe the IR and hence the 589 nm emission linewidth broaden with increasing laser power. We have measured with the same on-line OSA the 589 nm central linewidth for the powers of 10, 15 and 20 W CW and observe no changes (see Figure 14). The measured linewidth at 589 nm is 6.6MHz, without deconvolving the OSA instrument profile, and the line is symmetrical.

During a continuous 24 hours test, the average laser emitted power has been 20.4 W with an rms of 0.19W.

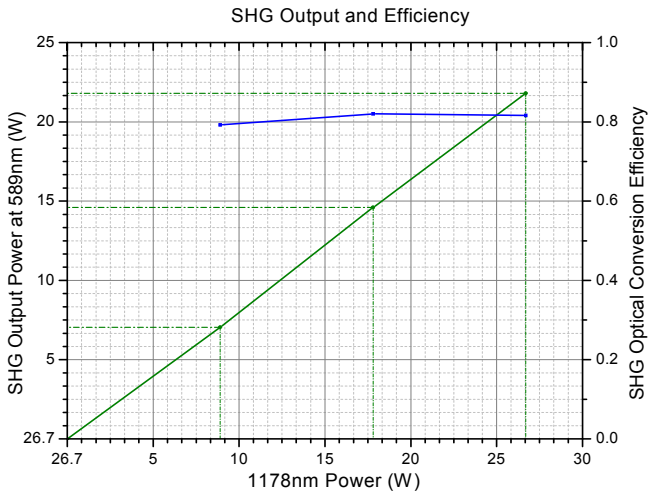

Figure 13: 589nm output power from the SHG-Pro ring cavity (left axis), as a function of input power at 1178nm. The conversion efficiency (right axis) is above 80% from 13W input onward.

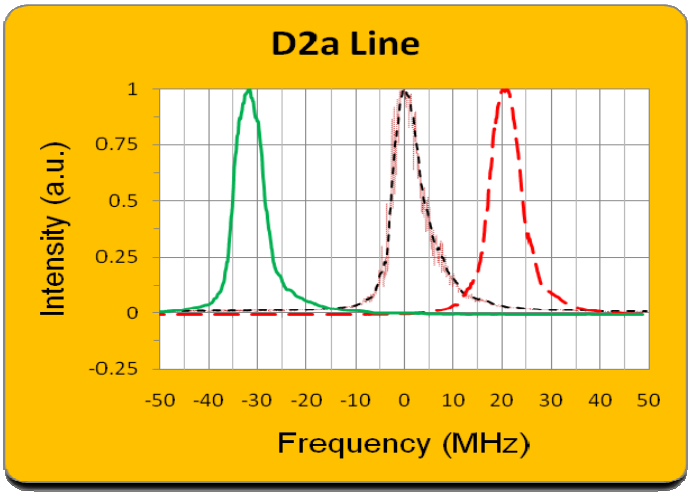

Figure 14: Laser spectrum at 589 nm. Three measured emission lines are shown, taken (from left to right) at 10, 15 and 20W emission power. The lines have arbitrarily shifted on the plot in order to see them, while keeping the frequency scale.

3.3 D_{2b} line generation

Through the phase variations induced by radio-frequency at 1.713 GHz applied to a 5mm aperture Electro-Optic Modulator crystal, a fraction of the fundamental 589 nm line photons are shifted by 1.713 GHz towards the red or the blue. The laser emission spectrum gets two sideband lines, the amplitude being determined by the RF power.

Those photons shifted toward the blue are exciting D_{2b} line transitions of the same sodium atom, and act as re-pumping photons [1].

We propagate a 2.5mm beam through the EOM to avoid optical wavefront distortions. The EOM indeed introduces thermal lensing which changes with the applied power. The shortest lensing observed at 20 W was 5 m radius of curvature. Therefore the output beam of the laser head is strictly speaking collimated only at 20 W power, at lower powers the focus changes and it will have to be compensated by the launch telescope beam expander, which will have an offset calibrated vs laser power levels.

It has been confirmed by test that the EOM indeed generates the correct sidelobes which achieve the desired intensity levels for operation (12%). During the return flux tests we will be able to vary the D_{2b} re-pumping from 0% to 18% of the central line peak intensity (see Figure 15), and measure the corresponding return flux variation.

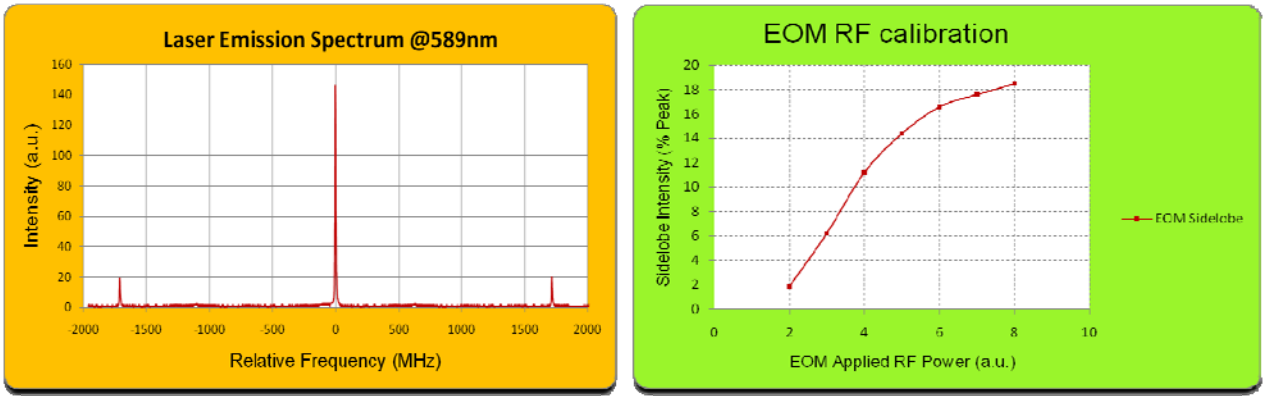

Figure 16: Laser emission spectrum with sidebands at 1.713 GHz (left). Varying the RF power applied the side-lobe intensity can be varied up to 18% in our setup (right). Both plots are experimental results obtained during tests of the laser head.

3.4 Wavelength Control

The laser wavelength control system uses a Toptica WSU/10 precision wavelength-meter with 10MHz absolute accuracy, and a stabilized TEM_{00} He-Ne laser as reference. It stabilizes the master oscillator wavelength at 1178 nm, which by frequency-doubling is directly linked to the 589 nm wavelength, avoiding therefore the use of a Sodium reference cell.

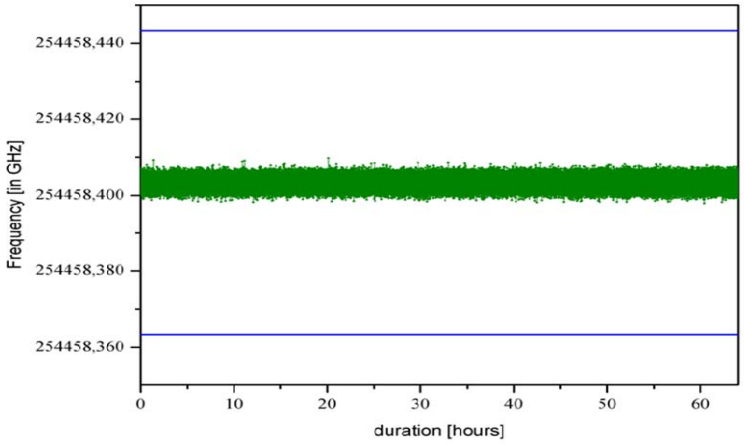

Figure 15: error signal of the laser wavelength control loop, for 64 hours of closed loop operation at 1178nm. The rms error is 2 MHz.

The wavelength control uses 0.5mW from the 1178 nm seed laser source at 2 Hz loop frequency. The laser emission frequency stability specification is ±40 MHz. A long term test carried over 64 hours has produced 2 MHz rms error (see Figure 16).

3.5 Laser Beam Optical Quality

The optical beam quality has been measured at 20 W with the EOM in operation and the AOM crystal in the beam path, not modulating, using a pick-off window at the exit of the laser head and a Haso Shack-Hartmann wavefront sensor. The Wavefront error rms after removing tilt and focus is 6 nm (see Figure 17).

3.6 Pulsed Operation

Using the Acousto-Optic Modulator for beam deflection and a blocking D-shaped mirror for the 0^{th} order deflection the laser emission can be pulsed by amplitude modulation.

We have tested the AOM up to the frequencies of 330kHz and 660kHz. To use such high frequency we have reduced the beam size in the AOM to 0.8 mm instead of 2 mm, which will be used for 3-5 kHz pulse frequencies, provoking a drop down to 60% of the AOM modulation efficiency. The peak power during the experiment was 12W, the rise time <0.1µs.

4. SUMMARY AND CONCLUSIONS

It is strategic for the next years to have reliable LGS return flux models validated experimentally, for the design of the future LGS-AO system. Building up from earlier fiber laser development, a transportable LGSU with a 20W fiber-based laser is being designed, assembled and tested this year at ESO, to conduct measurement campaigns in 2011 and 2012.

The design of the laser and of the launch telescope have many similarities with the AOF/4LGSF LGSU [9], hence a byproduct of this activity is also a risk reduction on the 4LGSF subsystems being built. The assembly of the 20 W laser has been completed and extensive test results prove that it meets and often exceeds the specifications. Further work is necessary this year to complete the transportable LGSU and to further test and ruggedize the system for field operation.

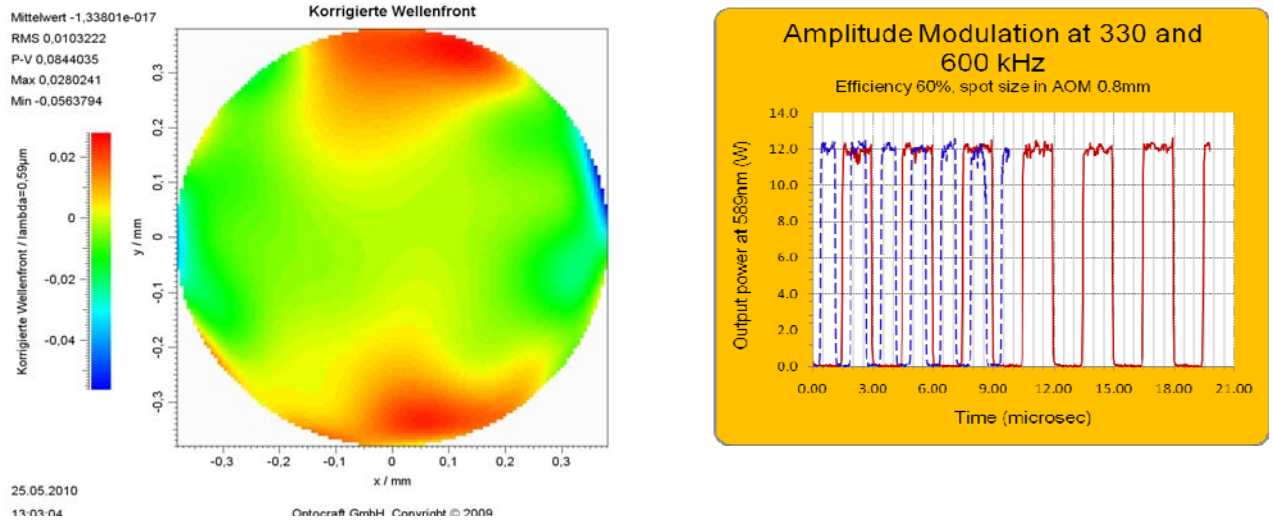

Figure 17: Left: wavefront measured at the exit of the laser head, with the laser at 20W, the EOM activated and the AOM crystal inserted in the optical path. The wavefront error is 6 nm rms. Tilt and Focus are removed. Right: Pulsed operation at 330 (solid line) and 660 kHz (dashed line). The pulse peak power is 12 W (60% modulation efficiency), the rise time is of the order of 0.1 microsecond. The modulation efficiency is reduced due to the small spot size on the AOM, necessary for this pulsed frequency.

REFERENCES

[1] Holzlöhner, R. , Rochester, S. M., Bonaccini Calia,D., Budker, D., Higbie, J. M. and Hackenberg, W., "Optimization of cw sodium laser guide star efficiency", Astron. & Astrophys. **510**, A20 (2010)

[2] Holzlöhner, R., Bonaccini Calia, D. and Hackenberg, W., "Physical Optics Modeling and Optimization of Laser Guide Star Propagation", Proc. SPIE **7015**, pp. 701521–701521-11 (2008)

[3] Pfrommer, T., Hickson, P. and She, C.-Y., "A large-aperture sodium fluorescence LIDAR with very high resolution for mesopause dynamics and adaptive optics studies", Geophys. Res. Lett. **36**, L15831, (2009)

[4] Moussaoui, N., Clemesha, B. R., Holzlöhner, R., Simonich, D. M. , Bonaccini Calia, D., Hackenberg, W. and Batista, P.P., "Statistics of the sodium layer parameters at low geographic latitude and its impact on adaptive-optics sodium laser guide star characteristics", Astron. & Astrophys. **511**, A31 (2010)

[5] Moussaoui, N., Holzlöhner, R., Hackenberg, W. and Bonaccini Calia, D. "Dependence of sodium laser guide star photon return on the geomagnetic field", Astron. & Astrophys. **501**, 793–799 (2009)

[6] Holzlöhner, R., Rochester, S. M., Pfrommer,T., Bonaccini Calia, D., Budker, D., Higbie, J.M. and Hackenberg, W.: "Laser Guide Star Return Flux Simulations Based on Observed Sodium Density Profiles", in Proc. SPIE **7736** in press (2010)

[7] Beckers, J.M.: "Adaptive optics for astronomy - Principles, performance, and applications" in Annual review of Astronomy and Astrophysics. Vol. 31 (A94-12726 02-90), p. 13-62. (1993)

[8] Arsenault, R. et al.: "Manufacturing the ESO Adaptive Optics Facility", in Proc. SPIE **7736**, in press (2010)

[9] Kaenders, W.G. et al. "Diode-seeded Fiber-Based Sodium Laser Guide Stars Ready for Deployment", in Proc. SPIE 7736-232, in press (2010)

[10] Taylor, L. R., Feng, Y. and Bonaccini Calia, D.: "50W CW visible laser source at 589nm obtained via frequency doubling of three coherently combined narrow-band Raman fibre amplifiers", Opt. Express, **18**, 8, 8540 (2010).